



Automated Canopy and Payload Motion Estimation Using Vision Based Methods

Ryan J. Decker,*

US Army Armament Research Development and Engineering Center, Picatinny Arsenal, NJ 07806

Oleg A. Yakimenko[†]

Naval Postgraduate School, Monterey, CA 93943-5107

This this paper advocates the use of automated computer vision and image processing techniques for characterization of parachute cargo systems. It considers two applications in which test video can be used to extract useful information about the behavior of these systems. The first application deals with identifying the relative motion of the decelerator canopy compared to that of the payload using a simple upward facing camera mounted on the top of the payload. The second application employs similar algorithms, but uses multiple ground-based cameras to reveal a six degree of freedom trajectory histories of parachute and parafoil-payload systems.

Abbreviations

2D/3D	= two / three dimensional
α_{sp}	= spatial angle of attack
θ_{sp}	= spatial pitch angle
ADS	= aerodynamic decelerator system
{ <i>c</i> }	= camera/image coordinate frame
CAD	= computer aided design
CCD	= charge-coupled device
CMDP	= Common Mission Debrief Program
COTS	= commercial off-the-shelf
FFT	= fast Fourier transform
GPS	= global positioning system
IMU	= inertial measurement unit
MEMS	= micro electromechanical systems
P	= position (xyz)
PADS	= precision air-drop system
RGB	= red-green-blue conventional color digital image
TSPI	= time space position information
SMD	= surface mount device
V	= velocity (xyz)
YPG	= Yuma Proving Ground, AZ

I. Background

Sophisticated instrumentation is usually required to characterize the parameters of an aerodynamic decelerator system (ADS). There are several conventional ways to approach the problem of quantifying the behavior of these systems. These include laboratory simulation, on-board instrumentation, and extensive manual video

* Mechanical Engineer, Fuze and Precision Armaments Technology, ryan.j.decker6.civ@mail.mil, Member AIAA.

[†] Professor, Department of Systems Engineering, Code SE/Yk, oayakime@nps.edu, Associate Fellow AIAA.

analysis. An example of a sophisticated on-board instrumentation is a sensor package developed for the ALEX systems by the Institute of Flight Systems of the German Aerospace Center (DLR) in the 90's [1,2]. Ref. [3] describes follow up efforts on instrumenting the FastWing system in the late 00's.

Due to the constraints of cost and weight, high-precision on-board instrumentation is not always an option for developmental ADS tests. Instead, many test ranges only employ simple global positioning system (GPS) recorders to record the descent trajectory. This can be problematic in terms of solution accuracy, and the use of GPS may not be sufficient to investigate the entire ADS trajectory from deployment to touchdown. Specifically, GPS data may not be available for the first ~30s of a parachute descent due to limited antenna visibility in the sky when released from a cargo aircraft. In addition, the high accelerations at canopy opening may saturate the GPS's oscillators introducing significant error in the trajectory results. That is where the use of an inertial measurement unit (IMU) on-board the payload has shown to be useful. The Payload Derived Position Acquisition System (PDPAS) being developed at Yuma Proving Ground (YPG) aims at closing this first 30s gap [4,5] by combining GPS data with an integrated IMU.

Relative motion between a parafoil canopy and the payload is also an important piece of information that cannot be measured using GPS. Quantifying this relative motion is essential for developing high-fidelity ADS models. This problem is complex, because most parachute and parafoil canopies are made of thin cloth material which makes it difficult to install bulky sensors that can accurately quantify motion. Most conventional means of measuring payload trajectories using on-board instrumentation cannot be used in conjunction with a parachute canopy without influencing the shape or behavior of the system. Instead, laboratory experiments have been conducted using near-range optical tracking systems such as the Vicon motion capturing system, which uses a network of grayscale or infrared camera systems to track the 3D motion of reflective markers in real-time [6, 7, 8]. Schoenenberger et al. [9] were able to use a laboratory camera system mounted in a wind tunnel to quantify the trim behavior of parachutes and measure important aerodynamic values such as the pitch damping and pitching moment coefficients through manual analysis of the video frames. The obvious limitation, however, of these laboratory simulations is relative to parachute drops, only very small segments of flight can be simulated within the enclosed and monitored test space.

As mentioned earlier, Ref. [1,2] studied the possibility of quantifying canopy motion by using a simple payload mounted digital camera positioned to look upward and capture video of the canopy while in flight on the ALEX system. Using computer vision algorithms, both the location and the orientation of the parachute were estimated. The FastWing program has also used this latter approach (back then a video camcorder was utilized, so that video data were digitized during a post-flight analysis).

Alternatively, miniature IMU devices can be installed at desired canopy locations to measure a variety of parameters for multiple canopy parts at the same time. One of these attempts was undertaken by Hur [10] where one single-axis and three tri-axial accelerometers were sewn into the main chord of the Buckeye paraglider along with a wireless transmitter. The entire setup including cables, connectors and batteries weighed 2.7 lb. A decade later, a much more consolidated and powerful system was developed that weighed only a few grams. For example, the VN-100 SMD (Surface-Mount Device) miniature high-performance IMU and Attitude Heading Reference System incorporates the latest micro-electromechanical systems (MEMS) sensor technology combining triaxial accelerometers, triaxial gyros, triaxial magnetic sensors, a barometric pressure sensor, and a 32-bit processor into a miniature surface mount module. Along with providing calibrated sensor measurements (at a rate of 100 Hz), this IMU/AHRS also computes and outputs a real-time, drift free 3D orientation solution that is continuous over the complete 360 degrees of motion. A similar system, the Bantam miniature IMU, which occupies only 1.7 in² and weighs 0.35 oz allowing it to be sewn in the smallest parafoil air-drop system (PADS) canopy, has been used in the study of comparing different fidelity models of PADS [11,12].

This paper addresses both aforementioned problems and presents the results of a preliminary study into using computer vision algorithms to characterize both canopy and payload motion from previously collected video. The paper is organized as follows; the next section describes efforts to use simple color segmentation algorithms to quantify canopy motion from a payload-based upward facing camera. The third section introduces research into using multiple ground-based video cameras to automatically quantify the descent trajectories of both the ADS canopy and payload. This is followed by research into measuring the relative motion between ADS canopies and payloads and the orientation history of the payload-canopy system. The final section of this paper contains the conclusions of this study.

III. Canopy Motion Characterization Using Payload-Mounted Cameras

A variety of tracking algorithms have been developed to identify and follow the motion of objects in digital video. These algorithms have been applied to video from upward facing cameras located on an ADS payload to quantify the relative canopy motion during an ADS descent. Some of these algorithms include sophisticated feature-based tracking methods that identify multiple key points, or simpler algorithms using color segmentation. For example, recent work by Hanke and Schenk [13] shows a strong potential to implement a photogrammetric approach with bundle adjustment software to find the relative orientation of canopy by tracking a set of markers. Figure 1 shows an example of some natural points that could be tracked. These include vertices formed by suspension lines, attachment points, and ribs endings at leading and trailing edges of the canopy.

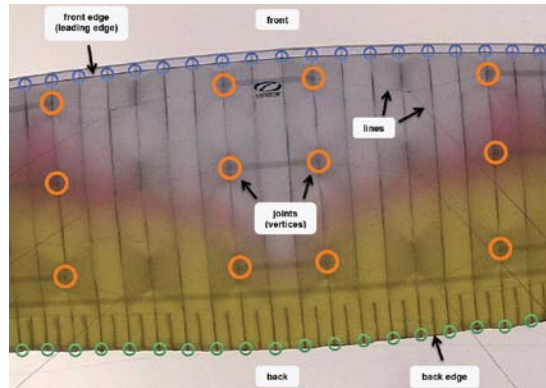


Figure 1. Natural points and features to track [Hanke and Schenk 2014].

Hanke and Schenk, Ref. [13], report that they used a calibrated 12 Megapixel Nikon D200 camera with 23.6×15.8 mm CCD (charge coupled device) taking high resolution 3872×2592 pixel images. Using PhotoModeler software they were able to reliably track the total of 270 points with only a few millimeters of error. This represents a significant breakthrough, because no modifications were made to the canopy, and “natural” points already existing on the parafoil canopy were able to be identified.

Similarly, the authors of this paper wanted to explore the feasibility of using color-segmentation techniques to describe the behavior of parafoil canopies without interfering with the natural canopy performance by adding reflectors or instruments. For years, the Naval Postgraduate School has been using commercial-off-the-shelf (COTS) parafoil canopies that come in a variety of colors for use with their Snowflake ADS [14]. During several of these drops, a Go-Pro Hero-2 digital camera was placed on the payload to monitor the behavior of the canopy to deliver 1920×1080 (1080p HD) video. Figure 2 shows the major steps of a simple color segmentation algorithm that finds and tracks a central red region of the Snowflake parafoil [15]. Beginning with a three-layer red-green-blue (RGB) digital color image for each video frame, a grayscale image is created using the red pixel layer subtracted by half of the sum of the blue and green layers. This simple conversion boosts the intensity of red pixels, while decreasing the intensity of green, blue, and white colors. From there, the resulting grayscale image is contrast-stretched and compared to a threshold value to generate a binary image containing mostly red pixels. The binary image then undergoes a sequence of morphological erode and dilation operations until only a single isolated body is produced that represents the largest concentration of red pixels.

Once the shape is isolated, the shape center is calculated as the average location of the segmented shape’s pixels (depicted in the last image in Fig.2 with a diamond marker). With just this shape isolated, the orientation of the shape can be estimated by calculating the inertial moment of the segmented shape’s pixels about the central moment. In Fig.3 the axis of the largest moment is depicted with an array of green star-shaped markers, while the transverse axis is shown with a black circle-shaped markers.

This color segmentation and shape analysis algorithm is processed on all frames of the canopy video during the descent. Once complete, the motion history if the canopy can be determined as shown in Fig. 4. Specifically, the data shown in Fig. 4 represents the relative displacement (X and Y in cm) of the canopy center and relative orientation (twist angle) of the canopy to the up-axis of the payload body.

This data can then be converted from the coordinate frame of the video camera ($\{c\}$) into a global reference frame by synchronizing the data from the other sources such as a payload-mounted GPS and IMU. Timing references for this synchronization can be done on the basis of events, which are registered in all sensor systems simultaneously such as the parafoil opening or landing event. Another option for data signal synchronization is the use of a dedicated time code that is generated by the onboard computer and recorded at the video as well.

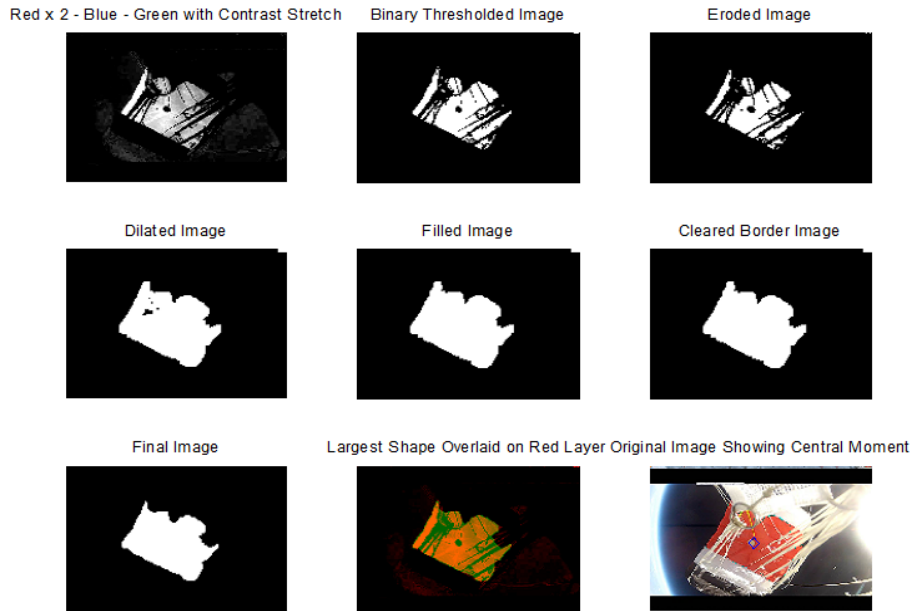


Figure 2. Isolating the red shape of the canopy.

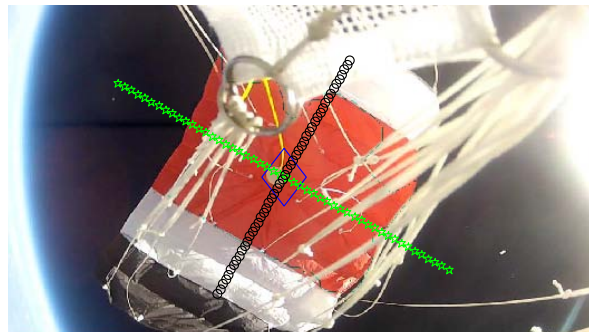


Figure 3. Proper identification of central moment and canopy orientation.

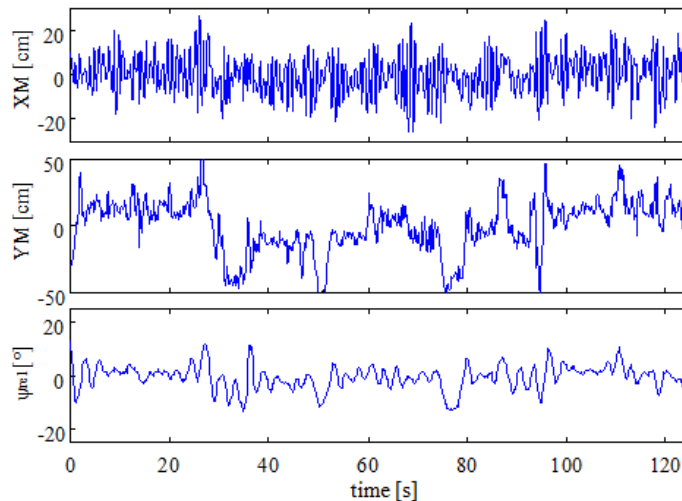


Figure 4. Measurement data of relative motion of the canopy.

From the preliminary experiments, the video analysis appears to be a promising tool that can supplement the payload based sensors and quantify the motion of the canopy as well. Of course, this method has drawbacks and challenges. The first challenge is to provide an uninterrupted view from the payload to the canopy by finding a suitable location to mount the video camera on the payload. On one hand, the camera must not disturb the parafoil deployment, while on the other hand, no obstacles such as reefing devices or harness straps should obstruct the view.

For many parafoil-payload systems, a wide angle lens is required to capture the whole canopy in the field of view and allow for accurate determination of the canopy center.

A major problem encountered with this algorithm is the sensitivity to lighting conditions. Changing illuminations and shadows cause difficulty for simple automated image processing algorithms. This often occurred during orientations where the sun appeared in the field of view. One solution for this problem is to guide the tracking manually through these difficult scenes. The same approach can be applied when the algorithm loses a tracked marker because of occlusions or because the canopy has traveled out of frame. An additional challenge with the proposed algorithm is that for certain tracking shapes (nearly square) the automated image processing algorithm may struggle to identify the forward direction of the canopy as compared to the lateral direction. As an example, Fig.5 shows a frame where the central red region being segmented by the color-tracking algorithm appears almost square in shape. To make matters worse, several detrimental effects occurred simultaneously such as occlusion and sun interference. As a result, the canopy shape was improperly segmented and the orientation was estimated poorly.

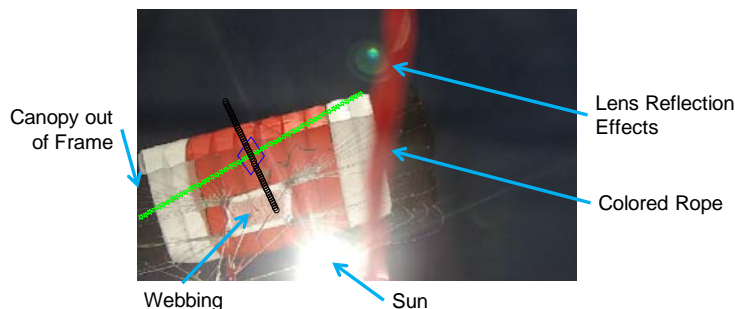


Figure 5. The causes of improper segmentation of canopy due to occlusion and other factors.

These issues were addressed in Ref. [15] where it was determined that from the practical standpoint, simply changing the canopy color configuration might be used to improve the robustness of the tracking algorithm (red and green colors would be the best choice to take a full advantage of RGB layering). Tracking multiple rectangular non-centered cells would be beneficial as well (Fig.6a). If one of these multiple regions could be a different color (Fig.6b), it would alleviate aliasing errors and therefore measure 360 degrees of canopy twist. To assess the potential accuracy of the improved color scheme shown in Fig.6b, a 3D canopy model was created using computer aided design (CAD) software. The resolution of the canopy images (400x600 pixels) was chosen to replicate the resolution from the Snowflake canopy video (recorded with a Go-Pro) and the background was set to use a gradient of blue similar to sky. After recording screenshots at various pre-determined orientations in the CAD model, the color segmentation algorithm was used to identify the colored regions and measure the canopy position and orientation as shown in Fig. 7. For this set of simulated canopy images, the highest error in twist angle measurement (relative to the commanded position in the CAD program) was only 0.24° , meaning that even at relatively low resolutions (compared to achievable test video), using two colored regions on a canopy are sufficient to determine the canopy twist angle and relative position to a payload-based camera.

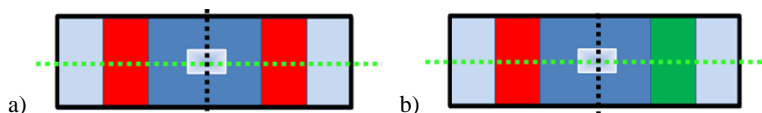


Figure 6. Improved canopy color configurations.

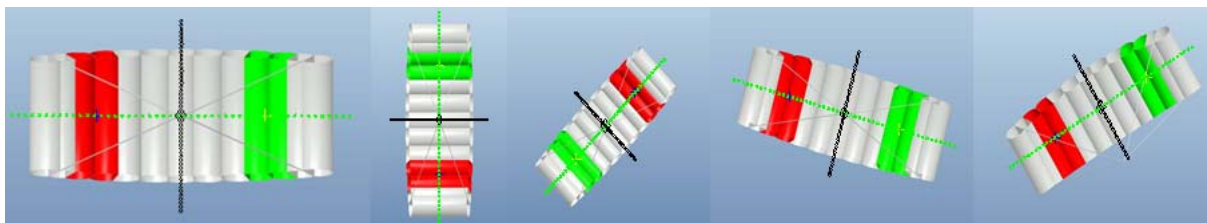


Figure 7. Sample analysis of 3D model generated images.

It should be mentioned that system identification is usually conducted at the earlier stages of PADS development when different color schemes for the canopy could be attempted. For a fielded PADS with monotonically colored canopies, attaching red or green patches to the underside of the canopy could enable the use of a color-segmentation based tracking algorithm.

III. Canopy – Payload System Analysis Using Ground-Base Cameras

During flight tests conducted at YPG, ADS video is often collected using multiple gimbale cameras capable of recording the relative azimuth and elevation histories during the ADS descent. Video data is manually post-processed to find x/y -offsets of the test article within the video frame. The azimuth, elevation, and x/y -offset histories are then conditioned and synchronized to find a time-space-position information (TSPI) solution. Traditionally, this process has been labor intensive and can take weeks to deliver the results from a single test.

An effort to improve the efficiency of the TSPI estimation has been undertaken using a telemetry protocol known as “Chapter 10” [16]. This protocol allows several streams of video and data to be time-synchronized and saved in a single data file. The software used at YPG to work with Chapter 10 data files is called the Common Mission Debrief Program (CMDP) [17]. A sample CMDP screenshot from a parachute drop is shown in Fig.8 that depicts all four view from the four ground-based camera systems used at the test site.

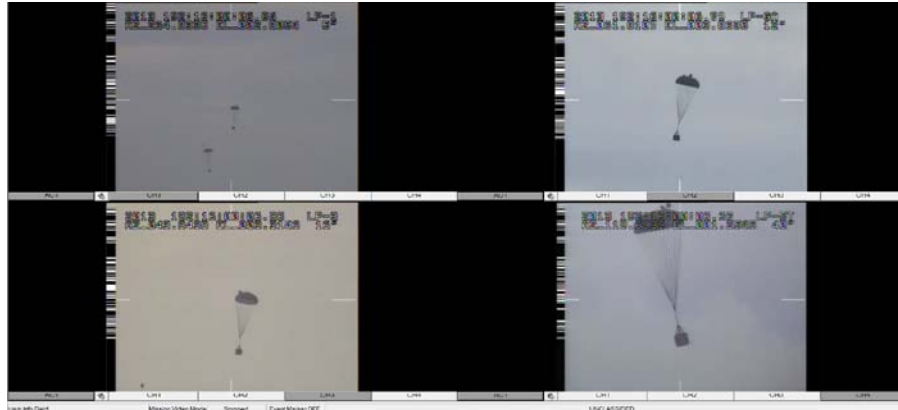


Figure 8. Common Mission Debrief Program displaying synchronized Chapter 10 data.

To further speed-up obtaining TSPI solutions and enhance the capability of tracking multiple objects (payload and canopy) several software packages could potentially be adopted. The TrackEye [18] motion analysis software is one such software package that can be used to track several specific features on the test object. These packages, however, still rely on a trained operator to manually find the object and initiate object tracking while monitoring a test video.

An automated algorithm similar to the one described in the previous section can be adjusted to handle automatic data extraction for both the payload and canopy. Instead of using the color segmentation algorithm, an edge detection-based method is used as described in Ref. [19]. Instead of tracking only the single largest object, the two largest objects are identified. As an example, Fig.9a shows both the canopy and payload being segmented and tracked simultaneously.

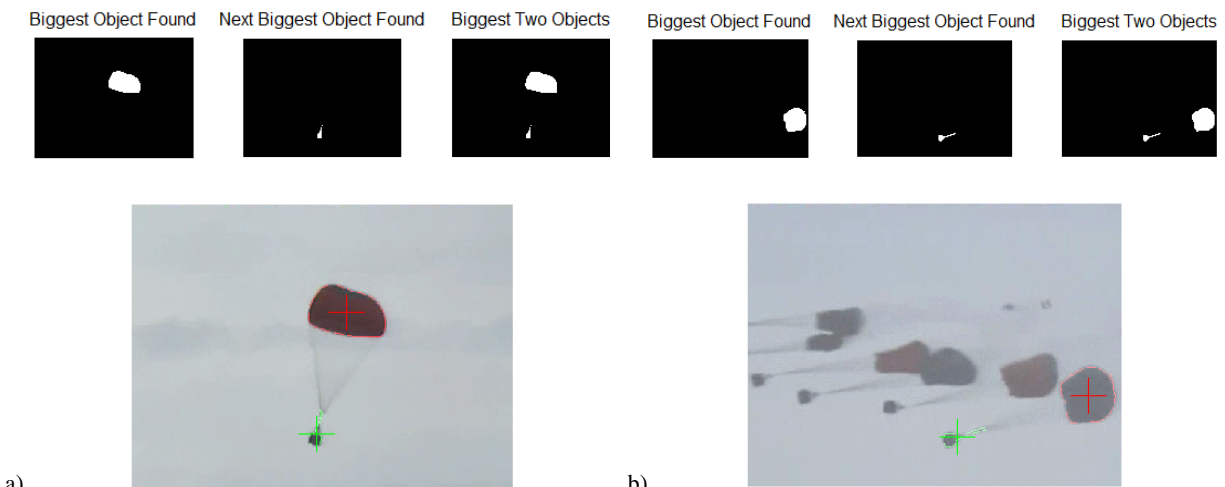


Figure 9. Parachute system dual object tracking for isolated system (a) and multiple systems (b).

The modified multi-stage algorithm starts by segmenting two shapes of a sufficient size in a given video frame. In order to reduce the probability of identifying the risers as pertaining to either the payload or the canopy shapes, the edge detection process starts at a low sensitivity and increases the sensitivity logarithmically until two large objects are found. Then, these objects are analyzed to see if they represent a parachute/payload system. Classification criteria involve the relative size and position of the objects. For example, the smaller object (candidate payload) should be between one quarter and one twentieth the size of the larger object (candidate canopy). Another criterion can be that the smaller object must appear below the larger object. If both objects are of sufficient size, the size ratio between them is acceptable, and the vertical positioning is correct, the two objects are classified as a payload and a canopy.

It should be noted that the particular classification criteria in terms of size ratio may be particular to the ADS being tested. The vertical position criterion should be used in cases where a drogue parachute body may be present above the main canopy. However, if the payload is wildly swinging around the canopy, as is sometimes the case during the first few moments of a turbulent deployment or during a maneuver in high wind as shown in Fig. 10a, the criterion of the payload appearing below the canopy shape could be relaxed. Additional criteria or more complex algorithms would be necessary to classify and track an increasing number of bodies as shown in Fig. 10b.

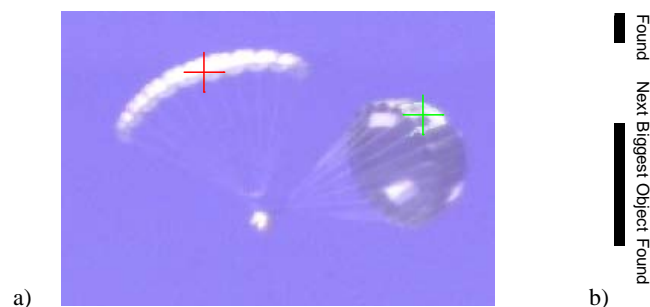


Figure 10. Difficulties in parafoil dual object tracking (a) and complex ADS shapes (b)

Once the system is classified, the second phase of the tracking algorithm is engaged. The image frame is separated into two parts, with one part focusing only on the canopy and the other focusing only on the payload. The new sub-image for the canopy is centered at the previously identified canopy center, and the size of the sub-image is chosen to be 150 percent of the distance between the previously identified canopy center and payload center. The payload sub-image is centered at the previously identified payload center, and the size of the window is chosen to be 50 percent of the distance between the previously identified canopy center and payload center. Each of these two windows is then resized to be 40×40 pixels for a common filtering operation which simulates a darkest-spot mean-shift tracking algorithm. The resized sub-image is inverted in intensity and filtered using a 5×5 pixel Gaussian kernel 20 times in a row until the jagged pixel intensity values resemble a smooth peak. The region surrounding this peak is used to fit a 2D paraboloid surface, and a sub-pixel estimate of the object center is found as the highest location on this peak. This process is illustrated for finding the payload center in Fig. 11. This same process is also conducted to find the center of the canopy sub-image.

The tracking algorithm proceeds frame-by-frame unless either object center has moved to the edge of the tracking window, or the center has moved more than a threshold distance from the previous center location. When this happens, the edge detection-based segmentation algorithm is re-initiated and the process restarts. An additional benefit of this automatically triggered process is that it could be used to track the parachutes during initial deployment when there are multiple parachutes present as illustrated in Fig. 9b. Instead of starting at the beginning of the video, the middle frame where the ADS is isolated can be analyzed first, and once the parachute and payload are identified, the video can be processed from the middle until the end, as well as from the middle backwards to the beginning.

IV. Results and Attitude Determination

Using the automated two-object scoring algorithm presented in the previous section it is possible to go beyond a simple TSPI solution described in the previous section and estimate the motion of parachute-payload system as a whole. As an example, Fig. 12a shows the payload and canopy centroids (in the image frame $\{c\}$) detected by the two-object scoring algorithm for one of three ground-based gimbaled cameras used in a low altitude descent from 980ft above ground level. Figure 14b presents pixel offset time histories for both objects with several obvious outliers removed using basic automated filtering operations.

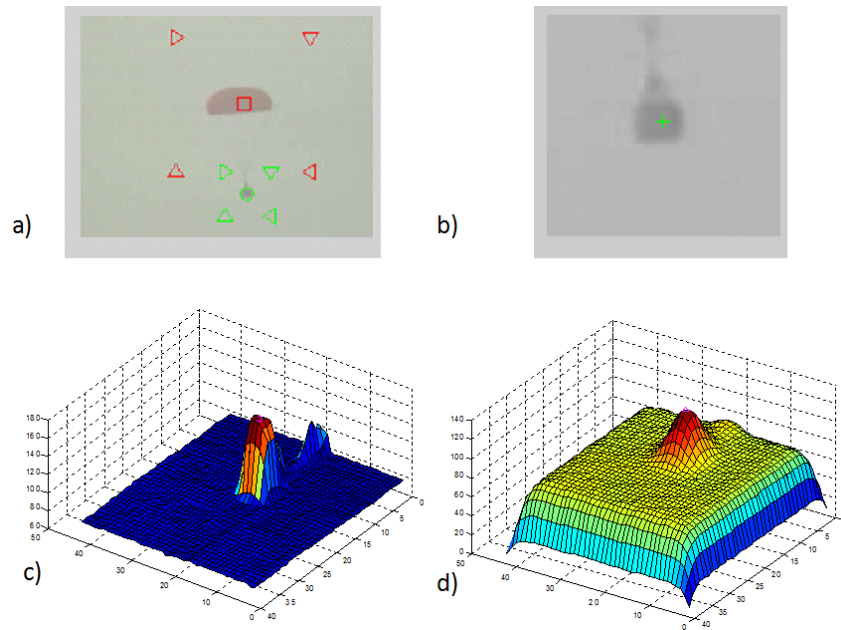


Figure 11. Parachute system tracking: original image (a) payload sub-image (b) resized and inverted sub-image (c) filtered sub-image (d).

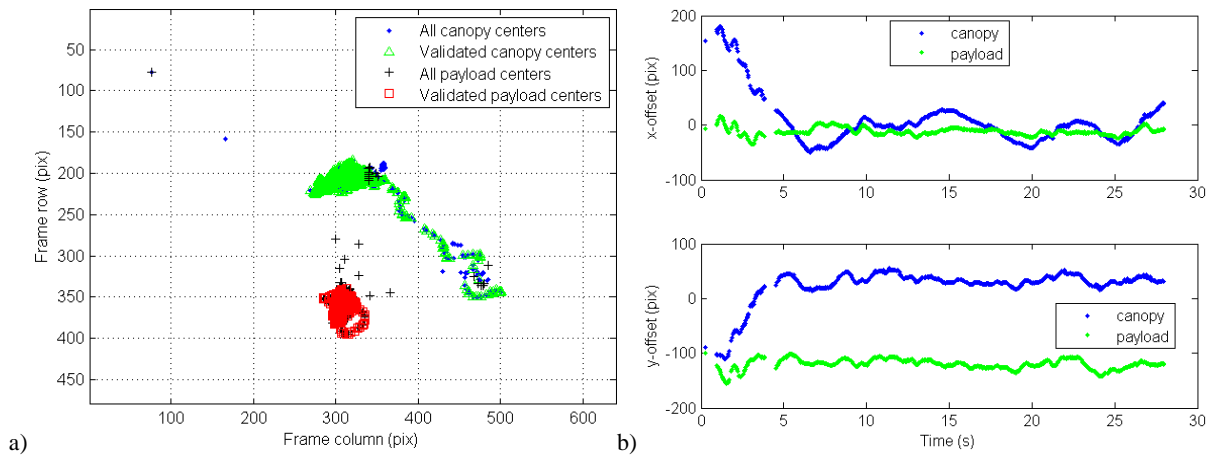


Figure 12. Plots of auto-scored canopy and payload pixel offsets $\{c\}$.

Figure 13 shows the result of a straightforward application of the dual-object tracking analysis to characterize the swinging motion of a payload-canopy ADS during its descent. Using differences between the x and y offsets of the canopy and payload centroids as seen by just one camera, the swaying motion of the parachute-payload system (swinging of payload relative to a canopy) can easily be retrieved. Obviously, the magnitudes shown in Fig.13 do not necessarily indicate the total swing angle of the payload, just the observed angle measurable in the image plane $\{c\}$. A fast Fourier transform (FFT) analysis of data presented in Fig.13 results in a peak oscillation frequency of 0.154 Hz, which corresponds to a median swing period T of about 6.5 s. This corresponds to the vertical dimension of the tested ADS, which in this case was about 34.5 ft, and the coupled roll-spiral mode data for a similar-size PADS. As seen from Fig.13a the distance between two centroids has a periodic behavior as well which may represent the natural frequency at which the parachute swells and releases air.

The data in Fig. 13b shows video analysis for the same ADS dropped from a higher altitude (with over 200 s of available video data). Again, the swinging motion exhibits very smooth periodic behavior (with only one grossly erroneous raw data point).

Essentially the same characteristics can be obtained by utilizing data from multiple cameras to produce a TSPI solution for both canopy and payload, $\mathbf{P}_{canopy}(t)$ and $\mathbf{P}_{payload}(t)$, respectively. Figure 14a shows the canopy-payload

distance and spatial pitch angle θ_{sp} (often referred to as the plumb angle) obtained by analyzing the difference $\Delta\mathbf{p}(t) = \mathbf{P}_{canopy}(t) - \mathbf{P}_{payload}(t)$. Figure 14b shows a horizontal projection of this vector (hodograph).

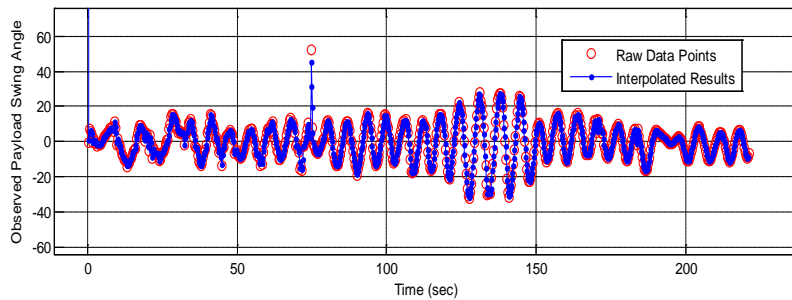
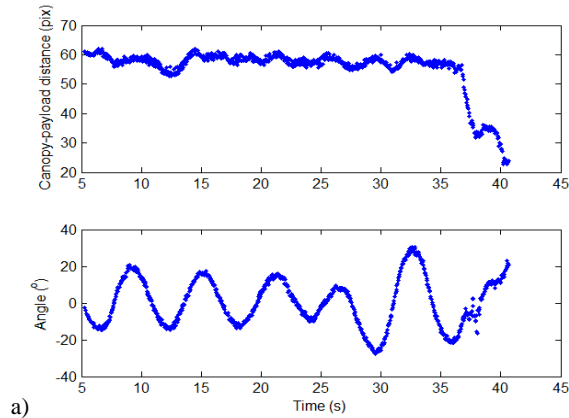


Figure 13. Distance between canopy and payload and ADS's attitude derived from Fig.14b data (a) and observed swing angle between payload and canopy in $\{c\}$ for a longer descent (b).

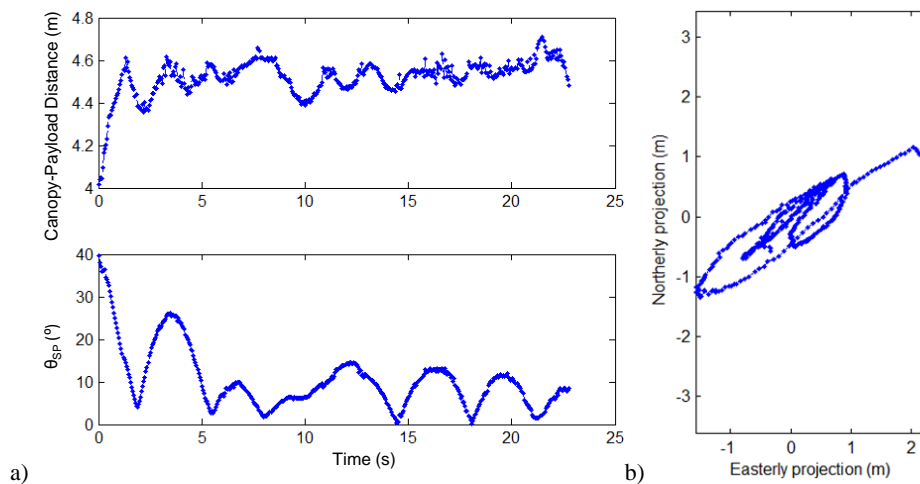


Fig.14 Canopy-payload distance and spatial pitch angle (a) and horizontal projection of $(x-y)$ position $\Delta\mathbf{p}(t)$ (b).

In order to compute the spatial angle of attack, α_{sp} , which is the angle difference between the longitudinal axis of canopy-payload system (θ_{sp}) and the system airspeed vector, the components of the airspeed vector need to be computed. To this end, differentiating the components of $\mathbf{P}_{canopy}(t)$ and $\mathbf{P}_{payload}(t)$ allows estimating the components of the groundspeed vector as shown in Fig.15. Figure 16 shows the difference between the canopy and payload groundspeed vector components characterizing a relative motion.

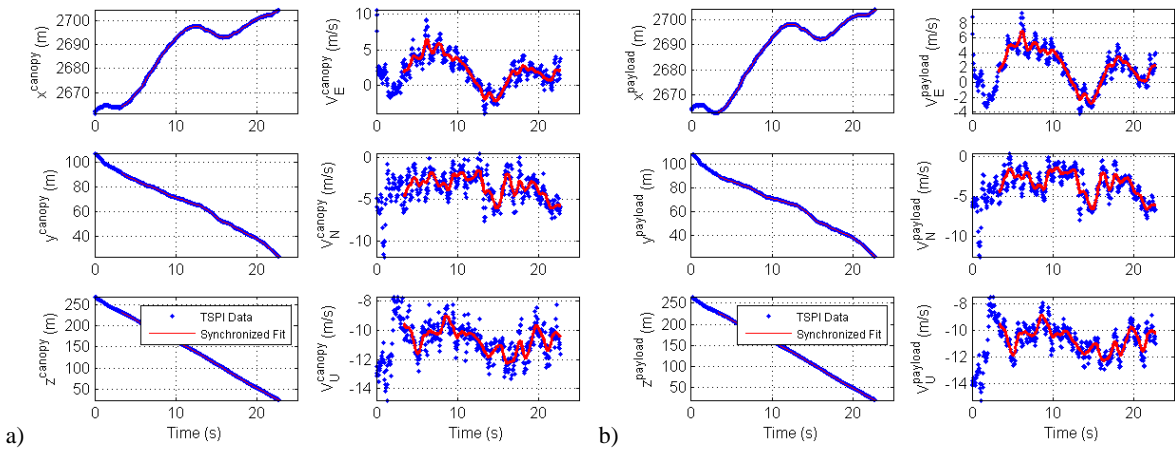


Figure 15. East, North, and Up components of the position and groundspeed vectors for canopy (a) and payload (b).

In order to use the data in Fig.15 to derive $\alpha_{sp}(t)$ the horizontal wind components should be subtracted from the canopy and payload groundspeed vector components to yield airspeed vector components. During test airdrops these winds are routinely measured and somewhat known.

For the short-duration low-altitude descent of the uncontrolled ADS corresponding to Fig.13 these winds were assumed constant and computed by averaging between the canopy and payload for the entire drop. Consequently, the mean values of the V_E and V_N groundspeed components, which happened to be $\bar{V}_E = 2.1m/s$ and $\bar{V}_N = 3.5m/s$, were subtracted from the Fig.15 data. Now that the airspeed vector was found, the spatial angle of attack can be computed. For the data analyzed in Figs.14-16, the $\alpha_{sp}(t)$ histories measured from both the canopy and payload are presented in Fig.17. For the payload, $\alpha_{sp}(t)$ happens to be slightly higher than for the canopy which make physical sense because the swinging causes the payload to have higher velocity magnitudes.

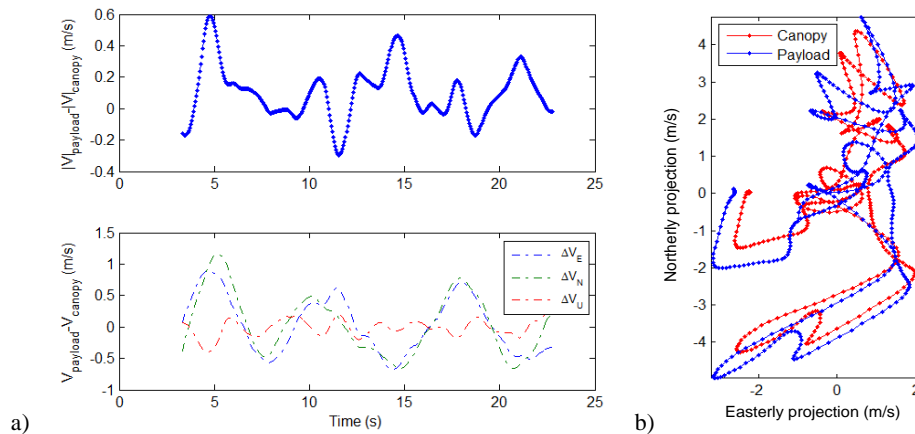


Figure 16. Difference between canopy and payload speed vector components (a) and horizontal projection of the airspeed vector for canopy and payload (b).

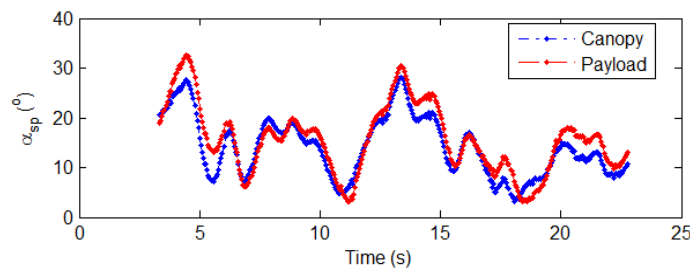


Figure 17. Spatial angle of attack for canopy and payload.

V. Conclusions

This paper presents two different types of analysis in which computer vision algorithms can be used to characterize the motion of a parachute-payload ADS. An approach was outlined for analyzing video from a payload-mounted camera as a simple way to describe the motion of a parafoil canopy relative to the payload system. The results show promise, but unfortunately a lack of sample video with an adequate view of the canopy prevented a complete assessment. Computer modeling has shown that if an optimally colored canopy was used and occlusion was reduced, the relative canopy motion could be measured with reasonable accuracy.

Ground based cameras have been used for decades to measure ADS descents. The approach discussed in this report is novel in that it allows simultaneous and fully automated analysis to measure the descent trajectory of an ADS when multiple cameras are available. For the first time, this allows important characterization metrics about the motion between the payload and the canopy to be computed in terms of relative position, velocity, and spatial orientation. Furthermore, the data can now be computed in minutes as opposed to waiting weeks for manually processed results. Further testing of this algorithm is planned along with a detailed accuracy comparison to high-precision differential GPS trajectory estimates.

Acknowledgements

The authors would like to thank Mike Diehl, Ryan Tiaden, and John Curry at Yuma Proving Ground (YPG), as well as Dr. Travis Fields at the University of Missouri-Kansas City for providing video data samples and collaborating to develop and validate video processing algorithms. They would also like to thank YPG and the Consortium for Robotics and Unmanned Systems Education at the Naval Postgraduate School for partially funding this research.

References

- ¹Jann, T., Doherr, K., and Gockel, W., "Parafoil Test Vehicle ALEX – Further Development and Flight Test Results," AIAA-1999-1751, *Proceeding of the 15th CEAS/AIAA Aerodynamic Decelerator Systems Technology Conference*, Toulouse, France, 1999.
- ²Jann, T., "Aerodynamic Model Identification and GNC Design for the Parafoil-Load System ALEX," AIAA-2001-2015, *Proceedings of the 16th AIAA Aerodynamic Decelerator Systems Technology Conference*, Boston, MA, 2001.
- ³Jann, T., and Greiner-Perth, C., "Flight Test Instrumentation for Evaluation of the FASTWing CL System," AIAA-2009-2932, *Proceeding of the 20th AIAA Aerodynamic Decelerator Systems Technology Conference*, Seattle, WA, 2009.
- ⁴Tiaden, R.D. and Yakimenko, O.A., "Concept Refinement of a Payload Derived Position Acquisition System for Parachute Recovery Systems," *Proceedings of the 20th AIAA Aerodynamic Decelerator Systems Technology Conference and Seminar*, Seattle, WA, 2009.
- ⁵Tiaden, R.D., "Payload Derived Position Acquisition System (PDPAS) Algorithm Implementation with the Common Range Integrated Instrumentation System Rapid Prototype Initiative (CRIIS-RPI)," *Proceedings of the 21st AIAA Aerodynamic Decelerator Systems Technology Conference and Seminar*, Dublin, Ireland, 2011.
- ⁶Gonyea, K., Braun, R., Tanner, C.L., Clark, I.G., Kushner, L.K., and Schairer, E., "Aerodynamic Stability and Performance of Next-Generation Parachutes for Mars Entry, Descent, and Landing," AIAA 2013-1356, *Proceeding of the 22nd AIAA Aerodynamic Decelerator Systems Technology Conference and Seminar*, Daytona Beach, FL, 2013.
- ⁷Jones, T., Downey, J., Lunsford, C., Desabrais, K., and Noetscher, G., "Experimental Methods using Photogrammetric Techniques for Parachute Canopy Shape Measurements," *Proceedings of the 19th AIAA Aerodynamic Decelerator Systems Technology Conference and Seminar*, Williamsburg, VA, 2007.
- ⁸Tanner, C.L., Clark, I.G., Gallon, J.C., Rivellini, T.R., and Witkowski, A., "Aerodynamic Characterization of New Parachute Configurations for Low-Density Deceleration," AIAA 2013-1358, *Proceeding of the 22nd AIAA Aerodynamic Decelerator Systems Technology Conference and Seminar*, Daytona Beach, FL, 2013.
- ⁹Schoenenberger, M., Queen, E., and Cruz, J., "Parachute Aerodynamics from Video Data," *Proceedings of the 18th AIAA Decelerator Systems Technology Conference and Seminar*, Munich, Germany, 2005.
- ¹⁰Hur, G., "Identification of Powered Parafoil-Vehicle Dynamics from Modelling and Flight Test Data," PhD Dissertation, Texas A&M University, TX, 2005.
- ¹¹Gorman, C.M., and Slegers, N.J., "Modeling of Parafoil-Payload Relative Yawing Motion on Autonomous Parafoils," AIAA 2011-2614, *Proceeding of the 21st AIAA Aerodynamic Decelerator Systems Technology Conference and Seminar*, Dublin, Ireland, 2011.
- ¹²Slegers, N., Scheuermann, E., Costello M., and Bergeron, K., "High Fidelity In-Flight Pressure and Inertial Canopy Sensing," *Proceeding of the 23rd AIAA Aerodynamic Decelerator Systems Technology Conference and Seminar*, Daytona Beach, FL, 2015.

¹³Hanke, K., and Schenk, S., "Evaluating the Geometric Shape of a Flying Paraglider," *ISPRS Technical Commission V Symposium*, Riva del Garda, Italy, 2014.

¹⁴Yakimenko, O.A., Slegers, N., Tiaden, R., "Development and Testing of the Miniature Aerial Delivery System Snowflake," in *Proceedings of the 20th AIAA Decelerator Systems Technology Conference and Seminar*, Seattle, WA, 2009.

¹⁵Decker, R., "A Computer Vision-Based Method for Artillery Launch Characterization," Doctoral Dissertation, Naval Postgraduate School, Monterey, CA, 2013.

¹⁶IRIG 106, "IRIG 106-07 Chapter 10 Programming Handbook," Range Commanders Council: Telemetry Group, White Sands Missile Range, NM, 2009.

¹⁷CMDP, Common Mission Debrief Program, USAF 846TSS/TSI, Eglin AFB, Ft. Walton Beach, 2013.

¹⁸TrackEye Motion Analysis Software, Photo-Sonics Inc., Burbank, CA, 2012.

¹⁹Decker, R., Kolsch, M., Yakimenko, O., "An Automated Method for Computer Vision Analysis of Cannon-Launched Artillery Video." *ASTM Journal of Testing and Evaluation*. Vol. 42. No. 5, 2013.